Proceedings of the ASME 2018 37th International Conference on Ocean, Offshore and Arctic Engineering
OMAE2018
June 17-22, 2018, Madrid, Spain

OMAE2018-77902

CODE-TO-CODE VERIFICATION OF END-ANCHORED FLOATING BRIDGE GLOBAL ANALYSIS

Thomas Viuff
Department of Marine Technology
Norwegian University of Science and Technology
Trondheim, Norway

Xu Xiang
Norwegian Public Roads Administration
Oslo, Norway

Bernt Leira
Department of Marine Technology
Norwegian University of Science and Technology
Trondheim, Norway

Ole Øiseth
Department of Structural Engineering
Norwegian University of Science and Technology
Trondheim, Norway

ABSTRACT

A code-to-code comparison of the dynamic characteristics of an end-anchored floating pontoon bridge is presented for two commercial software commonly used in the offshore industry, i.e. SIMO-RIFLEX and ORCAFLEX. Furthermore, a second comparison of the hydrodynamic properties of the floating pontoons are compared between two commercial Boundary Element Method software, i.e. AQWA and WADAM. The pontoons are modelled with an extended bottom to change the dynamic properties of the bridge structure. Viscous effects of this so-called heave plate is not considered in the study. The study shows good comparisons between the natural periods of the floating bridge structure and both software yield good convergence in the time domain. However, significant differences in the stochastic response has been found.

NOMENCLATURE

H_s Significant wave height.
T_p Wave spectrum peak period.
γ Wave spectrum peakedness parameter.
s Spreading exponent in the $\cos^s$ spreading function.
r_x Radius of gyration.
EA Axial stiffness.
EI_y Bending stiffness about weak axis.
EI_z Bending stiffness about strong axis.
GI_x Torsional stiffness.
θ_0 Main wave direction in the spreading function.
Δt Time step in dynamic simulation.
H_3 Pontoon heave first-order wave force transfer function.
A_{33} Pontoon heave-heave added mass.
B_{33} Pontoon heave-heave potential damping.
n_e Number of elements in bridge girder between each pontoon.
T_n Natural period for mode n.
ξ Structural damping ratio.
M_y Moment about weak girder axis.
z Vertical displacement.
$\ddot{z}$ Vertical acceleration.
C_{55} Hydrostatic stiffness in pitch.
A_w Waterplane area.
σ_x Standard deviation of response x.
$\overline{\sigma_x}$ Average standard deviation of response x.
γ_{int} Numerical time integration parameter.
β_{int} Numerical time integration parameter.

INTRODUCTION

Floating bridges have been used for several thousand years as temporary structures for military purposes [1] but was not designed to withstand the harsh environmental conditions. One example is the floating bridge built by the Roman Emperor Caligula around 40 AD in calm sea conditions. A few days after the finished construction a storm destroyed the bridge sinking more than 1,000 ships which lead to a great famine in Rome that year [2]. Only in recent decades has the design of floating bridges reached a level of certainty in load prediction and understanding of the dynamic behaviour of a floating structure, to be used as a reliable option in modern infrastructure. Examples of which are the First Bridge on Lake Washington (1940) and the Hood Canal Bridge (1958) in the United States, the Bergsøysund Bridge (1992) and the Nordhordland Bridge (1994) in Norway and more recently the Yumemai Bridge (2000) in Japan [1]. Of these examples, only the Hood Canal Bridge, the Bergsøysund Bridge and the Nordhordland Bridge are situated in rough sea conditions.

Today the Norwegian Public Roads Administration in Norway is planning to build multiple floating bridges along the E39 Coastal Highway Route due to the particularly deep and wide fjords. These special circumstances require reliable design tools and codes. Performing code-to-code verification of the numerical models is one way of making sure the design tool is reliable when existing software is applied to new problems.

METHODOLOGY

Two main comparisons are made in this study. First, a comparison of the Boundary Element Method (BEM) software WADAM [3] and AQWA [4] is performed, focusing on the hydrodynamic properties of the pontoons. Secondly, the stochastic response of the floating bridge is compared between ORCAFLEX [5] and SIMO-RIFLEX, of which the later is based on a coupled SIMO [6] and RIFLEX [7] analysis. Both numerical models are based on hydrodynamic properties calculated by WADAM and the focus is on the vertical displacement z, vertical acceleration $\ddot{z}$ and weak axis bending moment M_y of the girder. The stochastic response is influenced by the wave seed number in the generation of the wave loads. In order to minimize the effect of the random generation of the wave seed number the average values of 10×30 minutes simulations is used for each time a parameter is changed in the models. The parameters changed in the models are the time step Δt in the dynamic simulation, the number of elements n_e in the bridge girder between each pontoon axis and the main wave direction θ_0 in degrees.

In the following an overall description of the floating bridge structure is given followed by the comparison between the two BEM software. Later on a description of the modelling similarities and discrepancies is given for SIMO-RIFLEX and ORCAFLEX followed by a comparison of their respective performance in regards to natural periods, element and time step convergence and the stochastic response in beam sea and quartering sea. Unless otherwise stated the parameters listed above will be $\Delta t = 0.2$, $n_e = 10$ and $\theta_0 = 270^\circ$ for beam sea and $\theta_0 = 225^\circ$ for quartering sea. When specifying differences between the models in percentage, the values from ORCAFLEX is used as the reference.

FLOATING BRIDGE DESCRIPTION

The floating pontoon bridge is illustrated in Fig. 1 and consists of a single tower in South connected to the bridge girder with 4×20 stay-cables. To the North the bridge girder is resting on columns connected to 19 floating pontoons. The bridge has a horizontal radius of curvature of 5000 meter and an arc length of 4602 meter. The geometry and structural properties of the bridge is based on [8]. The tower has changing cross-sectional properties and goes from the bottom at a height of 5 meter to the top at 230 meter. The bottom of the tower is fixed in all degrees of freedom (DOF). The bridge girder, although in reality is made up of a twin-box cross-section, is modelled as a single equivalent beam along the entire length of the bridge with changing cross-sectional properties. The bridge girder is fixed at both ends, i.e. at AX22 and the first 60 meters from AX1. The height of the bridge is roughly 15 meters in North and 55 meters in South to allow for ship passage just North of the tower. The width of the girder and the connections to the stay-cables are taken into account by adding nodes perpendicular to the bridge girder axis, each with a distance of roughly 12 meter to the bridge girder axis. A rigid body connection between the bridge girder nodes and the adjacent nodes is utilized. The 80 pre-tensioned stay-cables connect the tower and the bridge girder and the length of the stay-cables range from 130 to 460 meter. The connection between the pontoons and the bridge girder is modelled with two columns positioned perpendicular to the bridge girder axis with a distance of 37 meter. The top of the columns are located 3.5 meter below the centroid of the bridge girder, due to the height of the bridge girder cross-section. The connections between the top of the columns and the bridge girder are modelled as a rigid body connections. The bottom of the columns are located at the top of the pontoons at a height of 4 meter where they are connected to the pontoons with rigid body connections. The pontoons are modelled as 6 DOF bodies located at the mean water level.

The pontoon panel model and the local- and global coordinate systems are illustrated in Fig. 2. The pontoon geometry is made up of a rectangular box in the middle, two half circle cylinders on each side and an extended bottom plate, which in the following will be refered to as a heave plate. The pontoon is 14.5 meter high, 28 meter wide and 68 meter long, and the heave plate is 5 meter wide and 0.6 meter high. All pontoons are given the same orientation with surge along the global x-axis (pointing towards North) and sway following the global y-axis (pointing

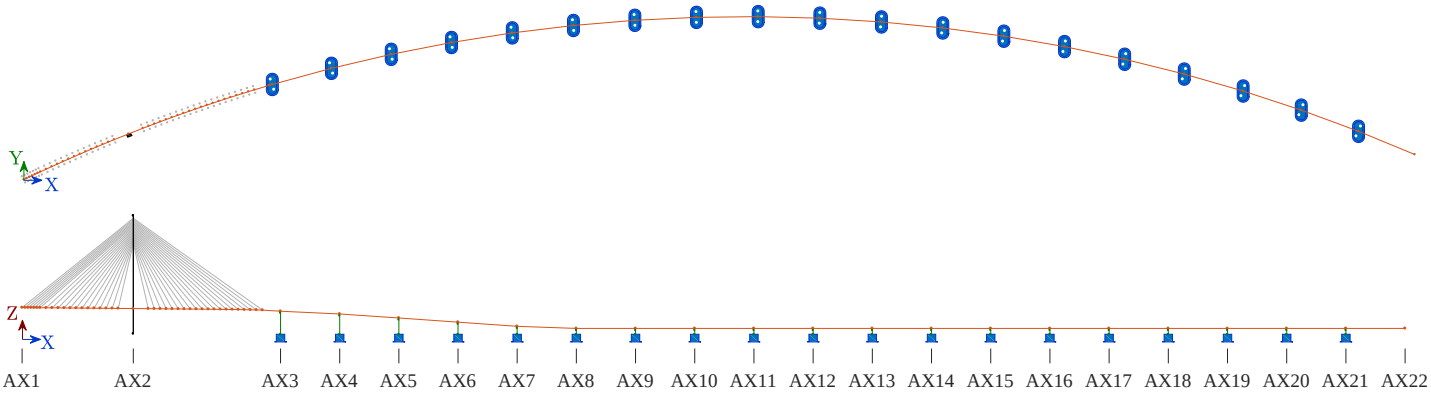

FIGURE 1. END-ANCHORED HORIZONTALLY CURVED FLOATING PONTOON BRIDGE SEEN FROM ABOVE (TOP) AND THE SIDE (BOTTOM)

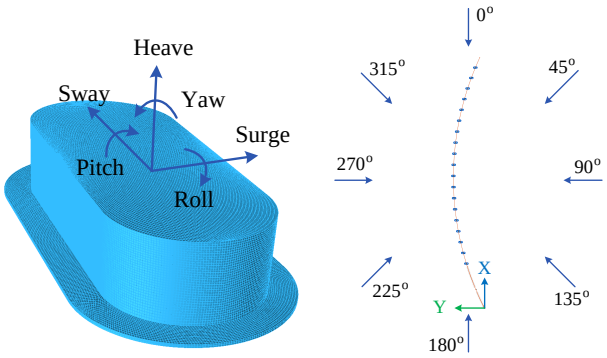

FIGURE 2. PONTOON COORDINATE SYSTEM (LEFT) AND WAVE DIRECTIONS (RIGHT)

towards West). The application of a heave plate on the pontoons is not a new concept but has been applied for many years in the offshore industry where it has been used to change the mass- and damping properties of structures such as floating wind turbines [9] or floating production storage and offloading (FPSO) units [10]. Although the viscous effects of the heave plate is not included in the current study, it is possible to do so if needed, see e.g. [11]. Ballast is added to the pontoons in order to keep them at the initial draft of 10.5 meter.

BEM SOFTWARE COMPARISON

The hydrodynamic properties of the pontoon is calculated in WADAM and AQWA with a draft of 10.5 meter. Both software are based on the theory and implementation of the boundary element software WAMIT. Although the number of panel elements is slightly different in the two models, the results from both software are based on mesh convergence. In WADAM a quarter panel model with 9061 panels are used and utilizes double-symmetry in the algorithm, whereas in AQWA a full panel model with roughly 22,000 panels are used. It should be noted that the numerical solution is not satisfied at sharp corners such as at the heave plate due to singularities [12]. This fact induces differences in the hydrodynamic properties of the pontoons. In both BEM software the height of the heave plate is covered by 2 panels.

The frequency-independent results such as the hydrostatic stiffness are very similar. As an example, in heave the difference is within 1 %. However, for the frequency-dependent results, i.e. added mass, potential damping and first-order wave load transfer functions, more significant differences can be observed. Figure 3 show the comparison of the two software for values in heave where differences of up to 5 % is found for heave added mass. The heave potential damping results show the same tendencies but with a slight shift along the wave periods. The largest difference (above 90 %) is between wave periods of 5.7 to 7.7 seconds and is mainly due to values being close to zero. At wave periods above 9 seconds the difference is decreasing from 44 % to 12 % and below 5.7 seconds the difference is for the most part less than 40 %. The first-order wave force transfer function for heave with waves from West show for the most part differences well below 10 %, although between periods of 6.3 to 8.3 seconds a difference between 20 % and 34 % exists. The differences in the hydrodynamic properties are possibly stemming from differences in mesh quality, particularly in regard to the sharp corners at the heave plate.

MODELLING THE FLOATING BRIDGE

Although the two software have origins in the same theoretical background, the modelling methods applied in SIMO-RIFLEX and ORCAFLEX have some differences. A description of the modelling considerations in both software is given in this section and a graphical representation of the two models can be

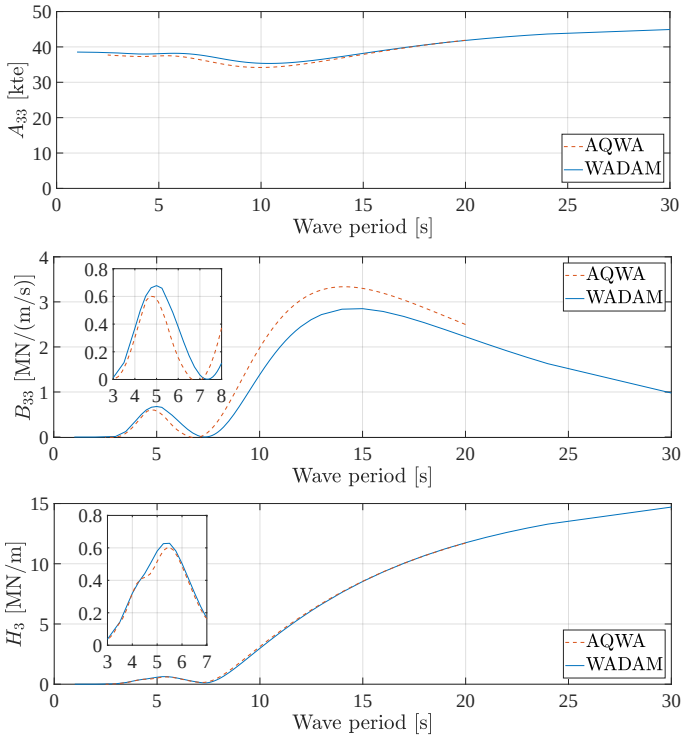

FIGURE 3. BEM SOFTWARE COMPARISON OF HEAVE ADDED MASS (TOP), HEAVE POTENTIAL DAMPING (MIDDLE) AND FIRST-ORDER WAVE LOAD IN HEAVE WITH WAVES FROM WEST (BOTTOM)

seen in Fig. 4. The main topology and cross-sectional properties are the same for both models and both models are given the same hydrodynamic input from WADAM for the pontoons.

Boundary Conditions

The girder node at AX2 is fixed in the global y-direction in SIMO-RIFLEX, whereas a relatively large linear spring stiffness is utilized in ORCAFLEX. The effect of this difference is expected to be relatively small. The nodes at AX1 and AX22 are fixed in the same way in both software.

Element Properties

In SIMO-RIFLEX the bridge girder and tower elements are modelled as Bernoulli-Euler beams based on small strain theory and includes stiffness contribution from geometric stiffness [13]. The stay cables are modelled as bar elements with no torsional stiffness. In ORCAFLEX the bridge girder, tower, columns and stay cables are all modelled as ORCAFLEX Lines. ORCAFLEX Lines consist of nodes connected by segments. The segments hold only axial and torsional properties whereas other loads, such as mass, buoyancy and drag forces are held by the nodes. Bending properties are represented by rotational springs and dampers at each end of a segment, between the segment and the node.

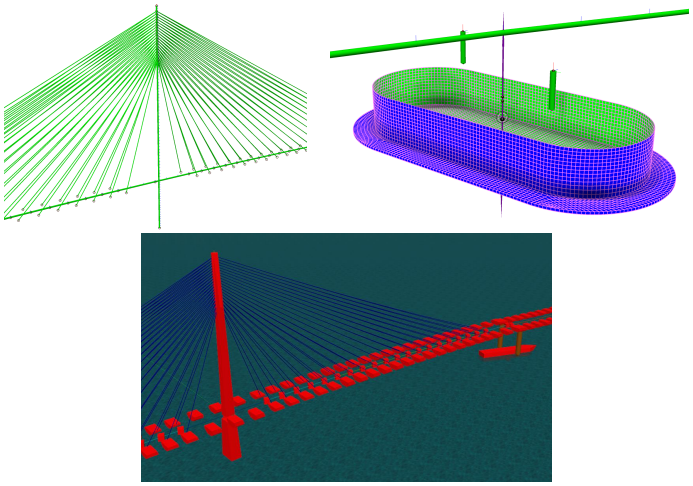

FIGURE 4. CONNECTIONS MODELLED IN SIMO-RIFLEX (TOP) AND ORCAFLEX (BOTTOM)

The two software uses different methods for incorporating the rotational mass moment of inertia of the elements. In SIMO-RIFLEX the property is specified by the corresponding radius of gyration, whereas ORCAFLEX calculates the values based on user specified ORCAFLEX 6 DOF Buoys with matching inertia properties and distances from the center line.

Table 1 lists the bridge girder cross-section properties in both models. The cross-section properties of the tower and the stay-cables are omitted due to the many different cross-sections. Instead the reader is referred to [8].

Pontoons and Connectivity

In ORCAFLEX the pontoons are modelled as ORCAFLEX Vessels and the connection between the pontoons and the columns are modelled with ORCAFLEX 6 DOF Buoys. Ballast is added to the pontoons by specifying an ORCAFLEX 6 DOF Buoy element at the position of the ballast. The calculation of the final pontoon mass matrix is handled by the software. The loads on each pontoon stems from the buoyancy force, the pontoon structural mass matrix, the hydrostatic stiffness matrix, first-order wave loads and frequency-dependent added mass and damping loads implemented through the retardation functions.

In SIMO-RIFLEX the pontoons are modelled as SIMO Bodies connected to a dummy line using Slender Element Connections. The dummy lines does not influence the structural properties but acts purely as a connection between SIMO and RIFLEX. Two different methods is used to include the buoyancy force in SIMO and RIFLEX. In SIMO the buoyancy force is included in the hydrostatic stiffness matrix and in RIFLEX the buoyancy

TABLE 1. PROPERTIES OF BRIDGE GIRDER CROSS-SECTIONS [8]. THE ROAD LINE BETWEEN AX1 AND AX3 IS DIVIDED INTO FIVE CONSECUTIVE SEGMENTS OF 220, 100, 100, 330 AND 10 METERS WITH CROSS-SECTION H1, H2, H3, H2, H1 AND S1, RESPECTIVELY. FROM AX3 TO AX22 ONLY CROSS-SECTION F1 IS PRESENT.

		H1	H2	H3	S1	F1
Mass	[te/m]	2.40E+01	2.91E+01	3.31E+01	3.18E+01	2.67E+01
r_x	[m]	1.66E+01	1.73E+01	1.76E+01	1.82E+01	1.76E+01
EA	[kN]	3.06E+08	4.41E+08	5.51E+08	5.25E+08	3.89E+08
EI_y	[kNm^2]	1.28E+09	1.98E+09	2.48E+09	3.85E+09	2.77E+09
EI_z	[kN^2]	1.16E+11	1.70E+11	2.12E+11	2.18E+11	1.55E+11
GI_x	[kN^2/rad]	1.42E+09	1.98E+09	2.48E+09	3.70E+09	2.90E+09

TABLE 2. PONTOON PROPERTIES WITHOUT BALLAST [8]

Property	Unit	Value
Mass	[te]	1.13E+04
Roll inertia	[tem^2]	4.90E+06
Pitch inertia	[tem^2]	1.36E+06
Yaw inertia	[tem^2]	5.70E+06
COG from waterline	[m]	-4.20E+00
Displacement	[te]	1.88E+04
Roll water plane stiffness	[kNm/rad]	3.98E+06
Pitch water plane stiffness	[kNm/rad]	7.38E+05
Heave stiffness	[kN/m]	1.74E+04

force is included in nodes using the Finite Element Method. In order not to include the effect of the buoyancy force twice, a specified force equal to the weight of the pontoon is added in the center of gravity pointing downwards along the global z-axis. Another specified force equal to the buoyancy force is added in the center of buoyancy pointing upwards along the global z-axis. The pitch and roll stiffness are then modified to only include the roll- and pitch water plane stiffness, e.g. $C_{55} = \rho g \iint_{A_w} x^2 \, dS$. Ballast is added to the pontoons by updating the elements in the structural mass matrix according to the ballast mass, mass moment of inertia and the distance from the center of gravity of the pontoon. Table 2 list the pontoon properties without ballast.

Standard Eigenvalue Solution Method

Both SIMO-RIFLEX and ORCAFLEX utilizes the Lanczos Method for solving the standard eigenvalue problem [5, 13].

Retardation Functions

The potential damping is used in SIMO-RIFLEX to calculate the retardation functions. In calculating the retardation function SIMO-RIFLEX also generates an added mass at infinite frequency matrix and an added linear damping matrix in order to compensate for the non-zero values at the truncation point of the retardation functions. In ORCAFLEX the same procedure is used to calculate the retardation functions, except no linear damping matrix is added to the system. The added mass at infinite frequency is taken from the frequency-dependent added mass input at the largest wave frequency.

Structural Damping

The structural damping is included in both software by specifying a mass proportional damping coefficient of 0.0025 and a stiffness proportional damping coefficient of 0.02. These coefficients yields a damping ratio $\xi < 0.02$ in the frequency range of the natural periods and the wave spectrum.

Time Integration Method

The time-domain analysis in SIMO-RIFLEX utilizes a step-by-step numerical integration scheme based on the Newmark β-family [13]. The integration parameters used is $\beta_{int} = 0.256$ and $\gamma_{int} = 0.505$ which will add small amounts of artificial damping to the system and help reach convergence faster in the time domain integration. The artificial damping has no measurable effect on the response.

TABLE 3. WAVE CHARACTERISTICS

Parameter	Unit	Value
H_s	[m]	3.0
T_p	[s]	5.6
γ	[-]	3.3
s	[-]	5.0

ORCAFLEX uses the implicit Generalised-α integration scheme to calculate the time domain response of the structure, which includes small amounts of numerical damping in order to damp out artificial, non-physical high frequency response inherent in the Finite Element Method [5]. This numerical damping should not have an effect on the accuracy of the results.

Wave Generation

In both SIMO-RIFLEX and ORCAFLEX the wave elevation is governed by the JONSWAP unidirectional wave spectrum and the cos^s spreading function. A list of the parameters for the two is given in Tab. 3. The randomness of the waves are controlled by the random wave seed number and the stochastic response given by the two software is thereby inherently different, although the same overall statistical properties are present.

COMPARISON OF BRIDGE NATURAL PERIODS

The comparison of the wet natural periods of the models are based on the case with $n_e = 10$ elements in the girder between each pontoon axis.

Both models utilize the iterative Lanczos algorithm for solving the standard eigenvalue problem (not including damping) and in both models the added mass at infinite frequency of the pontoons is added to the structural mass matrix of the pontoons. Table 4 lists the first 10 natural periods of the models and the difference between them in percentage. It is observed that the natural periods are relatively close to each other (within 6 %) with most of the natural periods within 3 % of each other. These relatively small margins indicate that the two software capture the same dynamic properties of the floating bridge structure.

CONVERGENCE STUDY IN BEAM SEA

Two convergence studies are carried out. First, convergence with respect to the number of elements in the bridge girder between each pontoon axis is investigated. Second, convergence with respect to the time step is carried out. Both studies are based on the case with $\theta_0 = 270^\circ$ representing beam sea from West and

TABLE 4. NATURAL PERIODS OF FLOATING BRIDGE

Mode	SIMO-RIFLEX	ORCAFLEX	Difference
n	T_n	T_n	
[-]	[s]	[s]	[%]
1	52.08	51.76	0.6
2	30.03	29.78	0.8
3	22.73	21.77	4.4
4	17.92	17.52	2.3
5	13.85	13.57	2.0
6	12.72	12.09	5.2
7	12.21	11.68	4.5
8	11.43	11.40	0.3
9	11.38	11.38	0.0
10	11.38	11.38	0.0

all other parameters are kept constant. The results shown are based on 10 simulations of 30 minutes for each time a parameter is changed and the convergence is evaluated by looking at the average standard deviation of the weak axis bending moment $\overline{\sigma_{M_y}}$ in the girder, for the girder node at bridge axis number 10, which is roughly in the middle of the bridge. Figure 5 shows the convergence results of the two studies.

Element Convergence

From AX3 to AX22 a single cross-section type is used, making it easier to do the convergence study of number of elements in the bridge girder. The number of elements in the bridge girder influences the number of modeshapes the structural model is able to capture in the simulation. With increasing number of elements an increasing number of modeshapes are captured. With this in mind the SIMO-RIFLEX Model and the ORCAFLEX Model both seem to convergence towards $\overline{\sigma_{M_y}} = 20$ MNm with increasing number of elements. Moreover, the decision to use $n_e = 10$ for the numerical study is verified by these findings.

Time Step Convergence

The convergence for both models with regards to the time step size shows clear convergence towards $\overline{\sigma_{M_y}} = 20$ MNm as the time step decreases. With regard to the time step size for the general analysis in the current study then it can be argued whether a time step larger than 0.2 could be used since the model seem to reach convergence at larger time steps. It should be noted

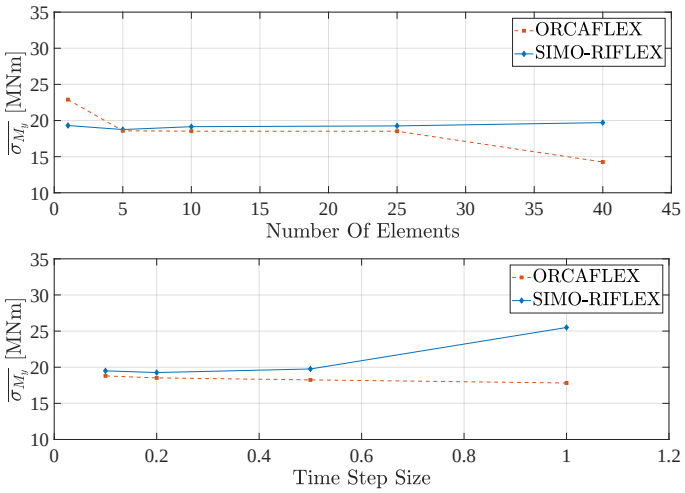

FIGURE 5. CONVERGENCE RESULTS OF STANDARD DEVIATION OF WEAK AXIS BENDING MOMENTS IN BRIDGE GIRDER AT AX10 FROM CHANGING NUMBER OF ELEMENTS (TOP) AND TIME STEP SIZE (BOTTOM)

however, that both the period and amplitude of the results are affected by the time step to period ratio and for time steps larger than 10 % of the period the period error is above roughly 8 % and the amplitude error is above roughly 3 % [14].

DYNAMIC RESULTS IN BEAM SEA

The comparison of the dynamic results is based on the case with $n_e = 10$ elements in the girder between each pontoon axis, a time step $\Delta t = 0.2$ seconds and a main wave direction of $\theta_0 = 270^\circ$ representing beam sea from West. The averaged extreme responses are based on 10 simulations of 30 minutes duration.

Figure 6 shows the maxima and minima of the dynamic vertical displacements, vertical accelerations and bending moment about the weak girder axis. Overall the two models show the same behaviour along the bridge axis, although the response values are off by an average of 11 % for vertical displacements, 13 % for vertical accelerations and 21 % for moment about the weak girder axis. The largest differences are located in the South end of the bridge near the high bridge part.

DYNAMIC RESULTS IN QUARTERING SEA

The comparison of the dynamic results is based on the case with $n_e = 10$ elements in the girder between each pontoon axis, a time step $\Delta t = 0.2$ seconds and a main wave direction of $\theta_0 = 225^\circ$ degrees representing quartering sea from South-West. The averaged extreme responses are based on 10 simulations of 30 minutes duration in order to minimize the influence from the

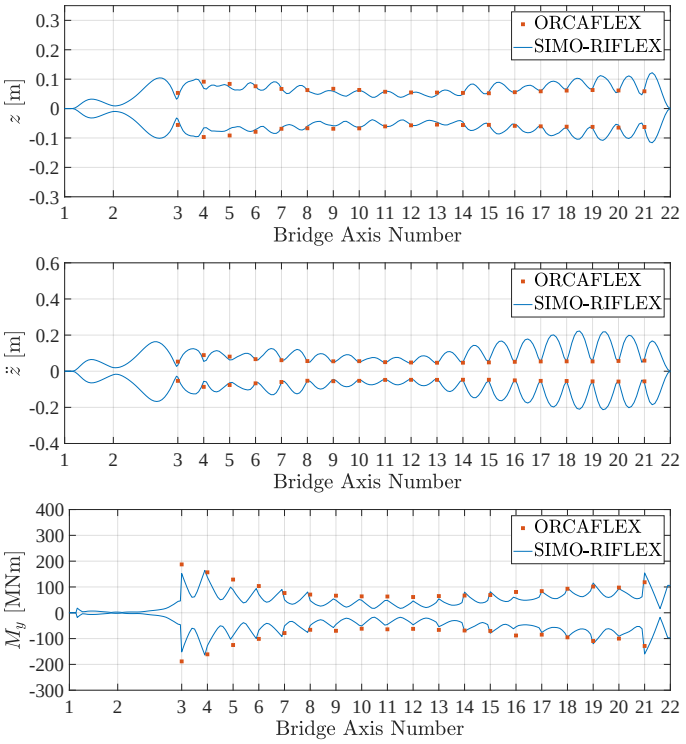

FIGURE 6. AVERAGE EXTREMA OF VERTICAL DISPLACEMENT (TOP), VERTICAL ACCELERATION (MIDDLE) AND BENDING MOMENT ABOUT THE WEAK GIRDER AXIS (BOTTOM) IN BEAM SEA FROM WEST

random wave seed number.

Figure 7 shows the maxima and minima of the dynamic vertical displacements, vertical accelerations and bending moment about the weak girder axis. Overall the two models again show the same behaviour along the bridge axis, although the response values are off by an average of 35 % for vertical displacements, 16 % for vertical accelerations and 12 % for moment about the weak girder axis. The largest differences of the displacements and the accelerations are located mainly in the sections from the middle to the North end of the bridge. The differences in the moments is more spread out along the bridge but again with smaller values around the high bridge part.

DISCUSSION

In spite of the natural periods indicating that the dynamic properties are the same in the two software, the stochastic response suggests otherwise. It is important to mention that the stochastic nature of the wave load has an impact on the average response values. Even though the effect of the random wave seed generation is minimized by taking the average of 10 runs with a simulation length of 30 min, the effect still persists in the results.

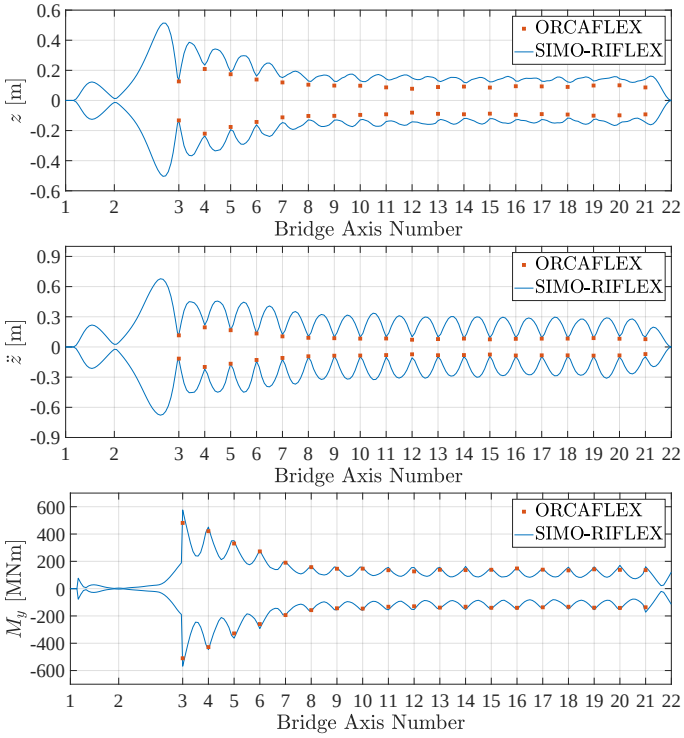

FIGURE 7. AVERAGE EXTREME VERTICAL DISPLACEMENT (TOP), VERTICAL ACCELERATION (MIDDLE) AND BENDING MOMENT ABOUT THE WEAK GIRDER AXIS (BOTTOM) IN QUARTERING SEA FROM SOUTH-WEST

Figure 8 illustrates this point by showing the standard deviation of the averaged maxima of the weak axis bending moments in SIMO-RIFLEX. The values are found from 5 sets of averaged maxima values. One averaged maximum value stems from a single set containing 10 runs with a simulation length of 30 min. The value of the standard deviations shown are equivalent to up to 7 % of the averaged maxima values for one set. This finding suggests that the randomness from the wave seed number is not entirely minimized and for a better comparison of the software used, a future investigation based on regular waves should be performed. This could also help shed more light on the variation of the differences observed along the bridge girder.

CONCLUSION

A code-to-code comparison of the dynamic characteristics of an end-anchored floating pontoon bridge is performed for two commercial software commonly used in the offshore industry, i.e. SIMO-RIFLEX and ORCAFLEX. The two models show overall the same behaviour in the vertical bridge response for beam sea from West and quartering sea from South-West. Average differences of 11 %, 13 % and 21 % is found in the vertical displacement, vertical accelerations and moment about the weak girder axis, respectively for beam sea from West. These differences change to 35 %, 16 % and 12 %, respectively, when the bridge is subjected to following beam sea from South-West. More importantly the differences along the bridge change between the two sea conditions.

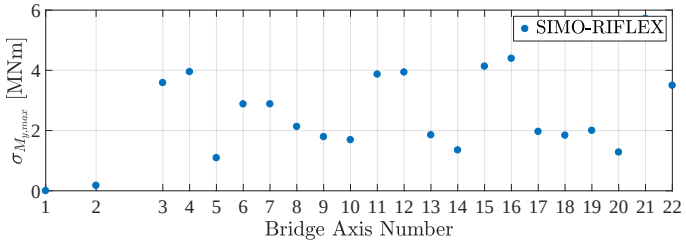

FIGURE 8. STANDARD DEVIATION OF AVERAGED MAXIMA WEAK AXIS BENDING MOMENTS IN BEAM SEA FROM WEST

A convergence study is carried out with regard to number of elements in the bridge girder and the time step size in the time domain calculation. Both models show clear convergence at 10 elements in the bridge girder between each pontoon and at a time step of 0.2 seconds.

Finally, a preliminary comparison of two Boundary Element Method software, i.e. AQWA and WADAM is performed, based on converged panel models. The preliminary comparison indicate relatively large discrepancies for the hydrodynamic properties in heave.

ACKNOWLEDGMENT

This research was carried out with financial support from the Coastal Highway Route E39 Project of the Norwegian Public Roads Administration. The authors greatly acknowledge this support.

REFERENCES

[1] Watanabe, E., 2003. "Floating Bridges : Past and Present Types of Floating Bridge". *Structural Engineering International,* ***2***, pp. 128–132.

[2] Graves, R., 1989. *I, Claudius*. Vintage Books, A Division of Random House, New York.

[3] Det Norske Veritas, 2014. *SESAM User Manual - Wadam*. Det Norske Veritas.

[4] ANSYS, Inc., 2012. *AQWA User Manual*. ANSYS, Inc.

[5] Orcina, 2018. Orcaflex documentation. `https://www.orcina.com/SoftwareProducts/OrcaFlex/Documentation/index.php`. Accessed 18/01/2018.

[6] SINTEF Ocean, 2017. *SIMO 4.10.0 User Guide*. SINTEF Ocean.

[7] SINTEF Ocean, 2017. *RIFLEX 4.10.0 User Guide*. SINTEF Ocean.
[8] Larsen, P., and et al., 2016. Curved bridge - navigation channel in south. Tech. rep., COWI and AAS-JAKOBSEN and GLOBAL MARITIME and Johs Holt as.
[9] Tao, L., and Cai, S., 2004. "Heave motion suppression of a Spar with a heave plate". *Ocean Engineering,* ***31***(5-6), pp. 669–692.
[10] Shao, Y.-l., You, J., and Glomnes, E. B., 2016. "Stochastic linearization and its application in motion analysis of cylindrical floating structure with bilge box". In Proceedings of the 35th International Conference on Ocean, Offshore and Arctic Engineering.
[11] Xiang, X., Svangstu, E., Nedrebø, Ø., Jakobsen, B., Eidem, M. E., Larsen, P. N., and Sørby, B., 2017. "Viscous damping modelling of floating bridge pontoons with heaving skirt and its impact on bridge girder bending moments". In Proceedings of the 36th International Conference on Ocean, Offshore and Arctic Engineering, pp. 1–10.
[12] Faltinsen, O. M. O. M., 1993. *Sea loads on ships and offshore structures*. Cambridge University Press.
[13] SINTEF Ocean, 2017. *RIFLEX 4.10.0 Theory Manual*. SINTEF Ocean.
[14] Langen, I., and Sigbjørnsson, R., 1979. *Dynamisk analyse av konstruksjoner: Dynamic analysis of structures*. Tapir.